

# RF MEMS switches based on thermal actuator

Huang Jiwei      Wang Zhigong

(Institute of RF- & OE-ICs, Southeast University, Nanjing 210096, China)

**Abstract:** A new switching circuit is presented for the application in the frequency range of 0 to 8 GHz. This switch is electro-thermally actuated and exhibits high radio frequency (RF) performance due to its lateral contact mechanism. It composes of electroplated nickel and silicon nitride as structural materials. The isolation between bias and signal ports is realized by using silicon nitride. In the case of a small deformation, the relation between the displacement of the vertex and the pre-bending angle is analyzed. The metal contact is realized by in-plane motion and sidewall connection. The switches were fabricated using the MetalMUMPs process from MEMSCAP. The RF testing results show that the switch has a low insertion loss of 0.9 dB at 8 GHz and a high isolation of 30 dB below 8 GHz.

**Key words:** RF MEMS (radio frequency micro-electro-mechanical systems); thermal actuator; lateral contact; isolation

Since the demonstration of Larson et al. in the early 1990's<sup>[1]</sup>, many researchers have reported MEMS (micro-electro-mechanical systems) switches for RF applications. These MEMS switches have a low insertion loss, a high isolation, a negligible power consumption, and a good linearity compared with traditional solid-state semiconductor switches. The majority of reported MEMS switches employ electrostatic actuation and operate with high actuation voltage, which makes them difficult to adapt for miniaturized mobile systems.

In this paper, a new switching circuit is presented for the application in the frequency range of DC 8 GHz. This switch is electro-thermally actuated and exhibits high RF performance due to its lateral contact mechanism. It is composed of electroplated nickel and silicon nitride as structural materials. Due to the insulation of silicon nitride, the isolation between bias and signal ports is realized. The metal contact is realized by in-plane motion and sidewall connection.

## 1 Structure and Principle

Fig.1 illustrates a schematic diagram of the proposed switch. It consists of a V-shaped beam, a contact head, an insulation dielectric connection and two signal lines. As an in-plane thermal actuator, the V-shaped beam is anchored at both ends, and buckled with a pre-bending angle  $\varphi$ . The electro-thermal actuator relies on the joule heating and resulting small mechanical ex-

pansion of the beams when a voltage is applied between the two anchors and a current is flowing through the beams. This effect actuates the contact head to move in the pre-bending direction through a silicon nitride connection. As a result, the in-plane motion of the contact head allows it to move forward and connect the RF signal lines via sidewall contact.

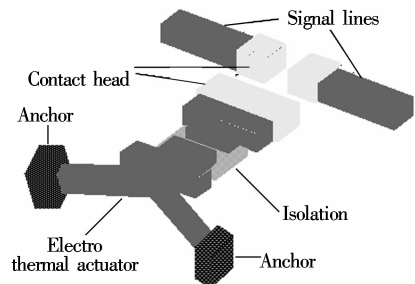


**Fig. 1** The schematic diagram of the switch

When V-shaped actuator beams are actuated by resistive heating, a rectilinear displacement and a large output force in the range of millinewtons can be received<sup>[2]</sup>. This will provide a stable and reliable contact with low contact resistance in the range of milliohms<sup>[3]</sup> and contribute further to obtaining high RF performance.

Fig. 2 shows a basic buckle-beam thermal actuator.



**Fig. 2** Basic buckle-beam thermal actuator

In our case the two boundary conditions are the same for both anchors. Suppose that  $L$  is the half length

Received 2007-05-09.

**Biographies:** Huang Jiwei (1976—), male, graduate; Wang Zhigong (corresponding author), male, doctor, professor, zgwang@seu.edu.cn.

of the beam and  $\Delta L$  is the expansion increment in the length of the beam. The total y-axis displacement of the actuator  $\Delta Y$  is given by

$$\begin{aligned}\Delta Y &= (L + \Delta L) \sin\left(\arccos\frac{L\cos\varphi}{L + \Delta L}\right) - L\sin\varphi = \\ &= (L + \Delta L) \sqrt{1 - \cos^2\left(\arccos\frac{L\cos\varphi}{L + \Delta L}\right)} - L\sin\varphi = \\ &= \sqrt{L^2\sin^2\varphi + 2\Delta LL + \Delta L^2} - L\sin\varphi\end{aligned}\quad (1)$$

It demonstrates the relation between the displacement  $\Delta Y$  and the pre-bending angle  $\varphi$ . To achieve maximal displacement, the differential equation is given by

$$\begin{aligned}\frac{d\Delta Y}{d\varphi} &= \frac{1}{2}(L^2\sin^2\varphi + 2\Delta LL + \Delta L^2)^{-\frac{1}{2}}(L^2 2\sin\varphi\cos\varphi) - \\ &= L\cos\varphi = \frac{1}{2}(L^2\sin^2\varphi + 2\Delta LL + \Delta L^2)^{-\frac{1}{2}} \cdot \\ &= (L^2 2\sin\varphi \sqrt{1 - \sin^2\varphi}) - L \sqrt{1 - \sin^2\varphi} = \\ &= L \sqrt{1 - \sin^2\varphi} = \left[ \frac{1}{\sqrt{\left(1 + \frac{2\Delta LL}{L^2\sin^2\varphi} + \frac{\Delta L^2}{L^2\sin^2\varphi}\right)}} - 1 \right] < 0\end{aligned}\quad (2)$$

So this function is descending, and it has the smaller angle and the larger displacement. Due to the process limit, the pre-buckle angle was chosen as  $1^\circ$ .

As shown in Fig. 3, buckle-beam actuators can be combined in an array, where the forces of each buckle-beam increase linearly. The displacement of the array is identical for the case of only one buckle beam, but the force will be much greater. This force of the actuator, for small displacements, can be approximated by the following expression <sup>[4]</sup>:

$$F = N \frac{Ew^3t}{4L^3} \Delta Y \quad (3)$$

where  $N$  is the number of actuators forming the array and  $\Delta Y$  is the displacement calculated in Eq. (1);  $E$ ,  $w$ ,  $t$  represent the Young's modulus, the width and the thickness of the beam, respectively. In this way, better contacts and lower ohmic losses can be obtained and lower switch insertion loss can be realized.

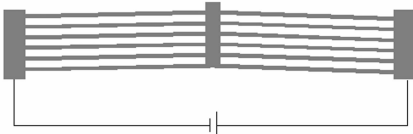


Fig. 3 The array of buckle-beam actuators

## 2 Contact Design

The MetalMUMPs process has a  $20\ \mu\text{m}$  thick electroplated Nickel and a  $1-3\ \mu\text{m}$  thick gold sidewall metal layer. Gold can be chosen as contact metal because of its low resistivity, good stability and efficiency

in RF signal propagation<sup>[5]</sup>.

The primary consideration for switch contact design is the contact area. A higher contact area usually has a lower constriction resistance and a lower contact temperature. True contact area and quality at this scale is determined primarily by the force and hardness of the contact material during plastic flow and its resistance to forming surface layers<sup>[6]</sup>. Different contact head shapes including square and angled have been designed to explore their reliability. The contact head area is designed after considering the tradeoff between contact resistance and load of silicon nitride connection.

According to the process rules, the closing gap between the contact head and the signal lines is  $8\ \mu\text{m}$ . Sidewall metal thickness of  $2\ \mu\text{m}$  is defined on both sides of the contact head to close the gap, which ensures a shorter expansion distance of the beam.

## 3 Process Technology

The switches were fabricated in the MetalMUMPs process from MEMSCAP. It is based on high resistive ( $\rho > 4\ \text{k}\Omega \cdot \text{cm}$ ),  $\langle 100 \rangle$  single crystal silicon wafers. Fig. 4 shows the fabrication process of the switch. First, a  $2\ \mu\text{m}$  layer of silicon oxide is grown on the wafer surface, as illustrated in Fig. 4(a). It is used as an isolation layer to reduce substrate loss. A  $0.5\ \mu\text{m}$  thick PSG layer, oxide 1, is deposited and patterned. It acts as a sacrificial release layer and defines the area that will be used to etch a trench in the silicon substrate. The  $0.35\ \mu\text{m}$  thick first nitride layer is deposited and patterned. Nitride 1 and the subsequent nitride 2 layers are used as an etching mask for the KOH etch and also serve as the structural connection as well as the electrical and thermal isolation between the driving structure and the contact structure. The results are shown in Figs. 4(b) and (c). Next, a  $1.1\ \mu\text{m}$  thick layer of the second oxide is deposited to release the nickel layer, as illustrated in Fig. 4(d). A  $20\ \mu\text{m}$  thick nickel layer is patterned using a thick photo-resist to form the stencil for the electroplated metal layer. The nickel layer is the main structure and the conductor layer for the switch, as shown in Fig. 4(e). After nickel plating, the resist plating mold is removed. Subsequently, a  $2\ \mu\text{m}$  thick gold layer is electroplated as sidewall metal to reduce electrical contact resistance in the contact area (see Fig. 4(f)). The last steps are the sacrificial layer releasing and the silicon trench etching. A wet chemical etch of the silicon, using KOH, is used to form a  $25\ \mu\text{m}$  deep trench in the silicon substrate<sup>[7-8]</sup>.

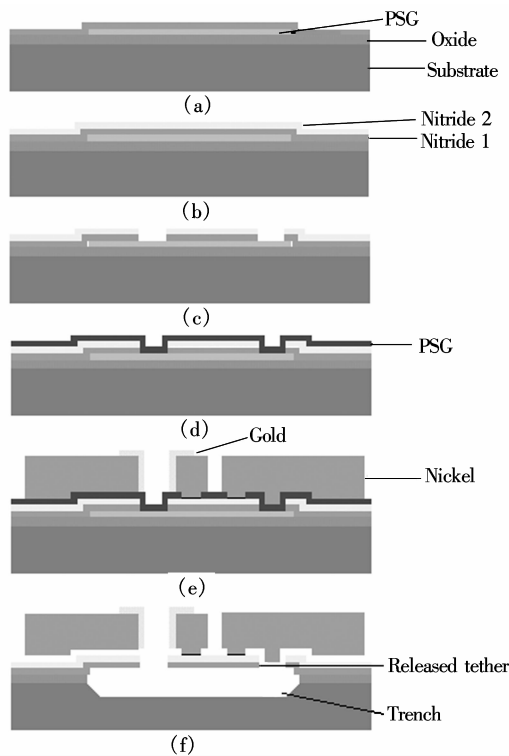


Fig. 4 Main fabrication procedures

ured off-state isolation is 30 dB at 8 GHz. The measurements also indicate that the switch has an insertion loss of less than 1 dB at 8 GHz.

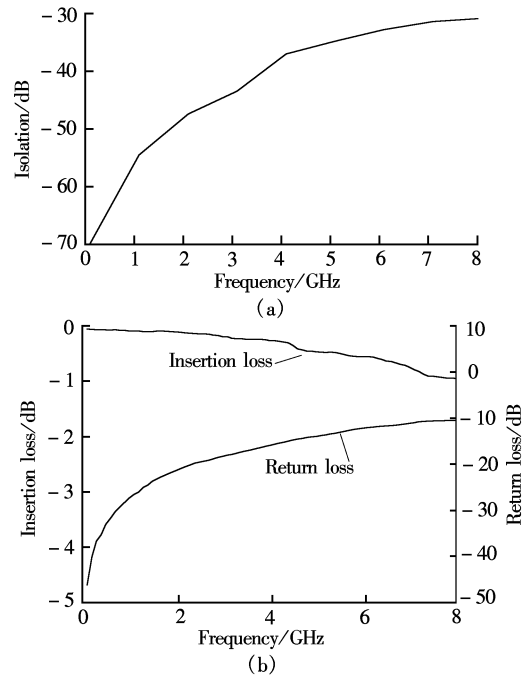


Fig. 6 RF performance of the switch. (a) Off-state; (b) On-state

4 Result and Discussion

Microphotographs of the fabricated switches are shown in Fig. 5. The chip area is 1 000  $\mu\text{m} \times 1\,300\, \mu\text{m}$ . On-wafer RF testing is performed using an Agilent PNA E8363B network analyzer and coplanar ground-signal-ground (GSG) microprobes with 150  $\mu\text{m}$  pitch. Calibration is done using a standard short-open-load-through (SOLT) calibration kit and parasitic of the testing pads are de-embedded. Fig. 6 shows that the meas-

DC testing shows that the switch can be operated at voltages of 0.5 to 1.0 V with contact resistance less than 0.6  $\Omega$ . Dynamic responses are measured using a function generator as the excitation source for the actuator and an oscilloscope monitoring the voltage at one terminal while the other terminal is supplied with a 1 V DC voltage. Fig. 7 plots the rising edge response time and the falling edge response time. The falling edge response time and the rising edge response time are measured to be less than 0.4 ms and 0.5 ms, respectively.

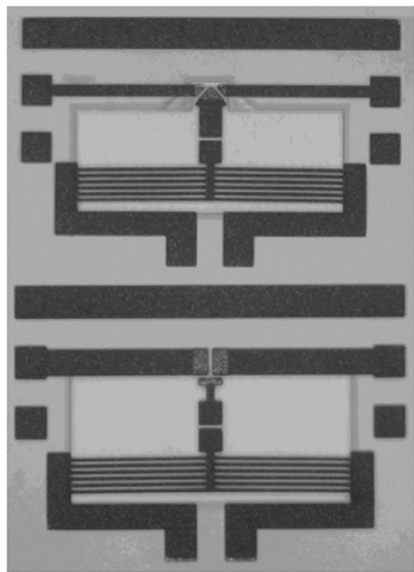


Fig. 5 SEM microphotograph of the fabricated RF MEMS switches

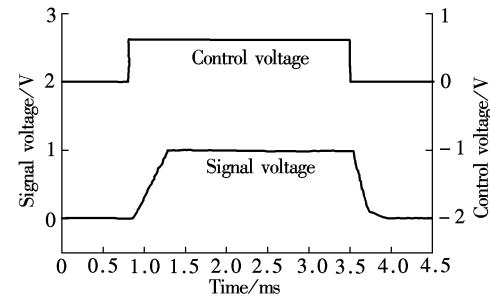


Fig. 7 Dynamic response of the switch

Contact heads with angled-shape showed better reliability than the square shape contact heads. It is easy and reliable to obtain the RF signal for angled-shape switches. The device exhibits a sub-ohm contact resistance. However, the signal is always difficultly achieved for a square-shape switch. And after running

several times, the head is detached from the isolation layer; as a result the square-shape switches were destroyed.

## 5 Conclusion

An RF MEMS switch with a thermal actuator has been fabricated on a high resistive  $\langle 100 \rangle$  single crystal silicon wafer. The switch relies on direct metal-to-metal contact to establish the RF signal path. RF testing results show that the switch has a low insertion loss of 0.9 dB at 8 GHz, and high isolation of 30 dB below 8 GHz.

## References

- [1] Larson L E, Hackett R H, Melendes M A, et al. Micromachined microwave actuator (MIMAC) technology—a new tuning approach for microwave integrated circuits [C]//*IEEE Microwave and Millimeter-Wave Monolithic Circuits Symposium*. Boston, MA, 1991: 27–30.
- [2] Que L, Park J-S, Gianchandani Y B, et al. Bent-beam electrothermal actuators—Part I: single beam and cascaded devices [J]. *IEEE Microelectromechanical Systems*, 2001, **10** (2): 247–262.
- [3] Hyman D, Mehregany M. Contact physics of gold microcontacts for MEMS switches [J]. *IEEE Trans Components and Packaging Technology*, 1999, **22**(3): 357–364.
- [4] Girbau D, Lkaro A, Pradell L. RF MEMS switches based on the buckle-beam thermal actuator [C]//*The 33rd European Microwave Conference*. Munich, 2003: 651–654.
- [5] Wang Ye, Li Zhihong, McCormick D T, et al. Low-voltage lateral-contact microrelays for RF applications [C]//*The Fifteenth IEEE International Conference on Micro Electro Mechanical Systems*. Las Vegas, NV, USA, 2002: 645–648.
- [6] Kruglick E J J, Pister K S J. Lateral MEMS microcontact considerations [J]. *Journal of Microelectromechanical Systems*, 1999, **8**(3): 264–271.
- [7] Cowen Allen, Mahadevan Ramaswamy, Johnson Stafford, et al. MetalMUMPs' s design handbook. Revision 2. 0. [R]. MEMSCAP, 2002.
- [8] Agrawal Vivek. A latching MEMS relay for DC and RF applications [C]//*Proceedings of the 50th IEEE Holm Conference on Electrical Contacts*. Seattle, WA, USA, 2004: 222–225.

# 热驱动式 RF MEMS 开关设计

黄继伟 王志功

(东南大学射频与光电集成电路研究所, 南京 210096)

**摘要:**设计了一种工作在 0~8 GHz 频段的热驱动式 RF MEMS 开关. 开关利用热驱动方式实现横向金属直接接触, 因此具有较好的射频性能. 开关的结构层由厚的电镀镍和氮化硅组成, 由于氮化硅的绝缘作用, 实现了射频信号与驱动信号的隔离, 有助于进一步提高射频性能. 分析了在较小变形量的情况下, 突起角度与顶点位移量的关系. 电镀的金壁作为接触金属降低了接触电阻. 开关通过 Metal-MUMPs 工艺进行成功流片, 测试结果显示, 开关在 8 GHz 有小于 0.9 dB 的插入损耗和大于 30 dB 的隔离度.

**关键词:**射频微机电系统; 热驱动器; 横向接触; 隔离

**中图分类号:** TN402